한국지진공학회 논문집 | 제11권 제4호 (통권 제56호) | 2007년 8월, pp. 25~31

Prediction of Strong Ground Motion in Moderate-Seismicity Regions Using Deterministic Earthquake Scenarios

강태섭[1]
Kang, Tae-Seob

ABSTRACT >> For areas such as the Korean Peninsula, which have moderate seismic activity but no available records of strong ground motion, synthetic seismograms can be used to evaluate ground motion without waiting for a strong earthquake. Such seismograms represent the estimated ground motions expected from a set of possible earthquake scenarios. Local site effects are especially important in assessing the seismic hazard and possible ground motion scenarios for a specific fault. The earthquake source and rupture dynamics can be described as a two-step process of rupture initiation and front propagation controlled by a frictional sliding mechanism. The seismic wavefield propagates through heterogeneous geological media and finally undergoes near-surface modulations such as amplification or deamplification. This is a complex system in which various scales of physical phenomena are integrated. A unified approach incorporates multi-scale problems of dynamic rupture, radiated wave propagation, and site effects into an all-in-one model using a three-dimensional, fourth-order, staggered-grid, finite-difference method. The method explains strong ground motions as products of complex systems that can be modified according to a variety of fine-scale rupture scenarios and friction models. A series of such deterministic earthquake scenarios can shed light on the kind of damage that would result and where it would be located.

Key words ground motion simulation, deterministic earthquake scenario, seismic hazard

1. INTRODUCTION

There are two standard types of seismic hazard analysis: deterministic and probabilistic. Specific earthquake scenarios are addressed using the deterministic model, whereas potential earthquake sources are considered using a probabilistic model. The two approaches, however, are actually mutually complementary. The deaggregation of probabilistic analysis results yields the magnitude and distance of a representative earthquake most likely to affect a given site. These parameters can then form the basis for a deterministic analysis. Through a simulation of deterministic earthquake scenarios, a data set for the response spectrum and ground motion time history at a site can be formulated. Because the data set represents a site-specific result, it can be used as a reference for the uniform hazard spectra and ground-motion relationships, which are the output and input of the probabilistic analysis. In this context, the concept of deterministic analysis is different from the conventionally accepted meaning.

Strong ground-motion records for recent seismic events have been gathered using dense seismic networks in seismically active areas such as North America, Japan, and Taiwan. For the Korean Peninsula, however, strong motion data are very rare, and the data available for destructive events consist of macroseismic intensities inferred from earthquake-related historical documents. For these situations, synthetic ground motions can be generated by taking into account the seismic source characteristics, the path, and the local geological and geotechnical conditions. The results can be validated against observed intensities before being used as the input in a subsequent seismic analysis (Panza et al. 2004).

[1] 정회원·한국지질자원연구원 지질연구센터 선임연구원
(대표저자: tskang@kigam.re.kr)

본 논문에 대한 토의를 2007년 10월 31일까지 학회로 보내 주시면 그 결과를 게재하겠습니다.

(논문접수일 : 2007. 7. 6 / 심사종료일 : 2007. 7. 30)

Earthquake ground motion is a coupled phenomenon that arises from fault rupture, propagation of the radiated wavefield, and site effects near the free surface. Characteristics of strong ground motions depend on the complicated interaction of these combined effects. Earthquake rupture includes dynamic processes of rupture nucleation, propagation, and healing that are governed by frictional properties at the fault surface. The seismic wavefield radiated by fault movement propagates through heterogeneous geological media and undergoes near-surface modulation by either amplification or deamplification. A complete understanding of these effects requires a numerical modeling technique with multi-scale resolution. High-resolution modeling with a dense grid and rapid time steps is required in the vicinity of the fault rupture to deal with the dynamic rupture processes. In contrast, modeling of the wavefield propagating through the media outside the rupture zone requires relatively low resolution. Even in the latter case, however, a large velocity contrast between media such as sedimentary basins surrounded by host rock forces modeling parameters to be discontinuous to avoid spatial and temporal oversampling in both time and space.

A three-dimensional, fourth-order, staggered-grid, finite-difference technique combining discontinuous grids with locally variable time steps (LVTS) was recently proposed (Kang and Baag 2004a,b).[2,3] The discontinuity of modeling parameters is generalized three-dimensionally such that a region of fine-scale modeling parameters can be localized within a larger domain and/or the boundary between the regions can be extended to the location of the free surface. These properties allow the LVTS scheme to be efficiently used for the modeling of both rupture dynamics and radiated wavefield in the heterogeneous media. Here I present a new approach to acquiring a general understanding of a complex system composed of source rupture processes, radiated wavefield propagation, and near-surface effects in a three-dimensionally heterogeneous Earth.

2. METHODS

2.1 LVTS Scheme

Kang and Baag (2004a,b)[2,3] introduced an LVTS scheme for simulating seismic wave propagation that matches with discontinuous grids used in the finite-difference method, presenting the computational core of the scheme and details of the computational procedures. The computational domain consists of two regions, each with different velocities, grid spacing, and time steps. Local discontinuous grids with three-times finer grid spacing in all three directions are also present (Fig. 1). Regions where fine and coarse sampling parameters overlap are called transitional zones. In a transitional zone, the wavefield is updated using two types of processes: exchange and interpolation. In the exchange process, nodes at the margin of one region are supplied with updated values for field variables computed by a finite-difference operator for the other region. In the interpolation process, for nodes where field variables that are not determined even by the exchange process in the finely sampled region, a spatial interpolation is applied using already known values for the two adjacent nodes in the coarsely sampled region. In the temporal domain, values for nodes along the outermost node line at the margin of the region with the smaller time steps are obtained by temporal interpolation using the known values for the coarsely sampled area and larger time steps immediately before and after.

2.2 Rupture Process

An earthquake is represented as a propagating stress

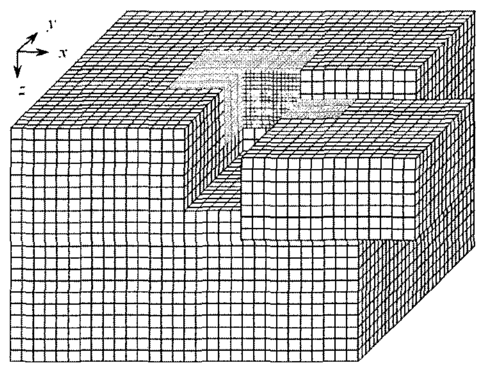

〈Figure 1〉 Schematic representation of a three-dimensional grid layout with localized discontinuous grids (Kang and Baag, 2004b). The model consists of two regions with different grid spacing that satisfy the local stability conditions based on minimum velocity in a specific region. Discontinuous grids have a three-dimensional blocky form that allows the boundary between regions to be extended to the Earth's free surface.

relaxation over a prescribed finite fault plane. Rupture initiates at a point on the fault and propagates circularly outward at a given velocity, v_r. When the rupture front reaches the prescribed boundary of the fault, the rupture suddenly stops. A simple friction model allows for sudden shear-stress decrease to a prescribed frictional stress when the rupture front reaches such a point on the fault. Source functions are generated dynamically as a result of propagating stress change, an important property that distinguishes dynamic modeling from kinematic modeling. Kinematic approaches are based on dislocation fault models for which the spatial and temporal source functions are predetermined because the stress state of the field is not fundamental information considered in such models. For this reason, dynamic rupture modeling is preferable in simulating strong ground motion based on a realistic fault model.

2.3 All-in-One Model for Simulation of Earthquake Phenomena

A three-dimensional blocky form of discretization can be used to model fault rupture and ground motions realistically and efficiently (Fig. 2). In the case of a near-surface sedimentary basin surrounded by bedrock (Fig. 1), high-resolution grids and time steps are used in the vicinity of the fault rupture to deal with the dynamic rupture processes. Madariaga et al. (1998)[6] discussed the selection of an appropriate sampling grid size to be discretized for a fault rupture domain with the aim of lessening numerical dispersion. Time steps are determined based on the stability conditions between grid size and time step for numerical simulation. Grids and time steps near the fault region are gradually refined until sufficiently high resolution is achieved to model the faulting processes realistically.

3. NUMERICAL EXAMPLES

3.1 Self-Similar Crack Propagation

Theoretical studies of relationships between strong ground motion and earthquake source parameters depict the earthquake as propagating dislocations. Here, numerical solutions for the case of circular rupture propagation are calculated. To simulate dynamic rupture, the technique of Madariaga et al. (1998)[6] is used, based on the fourth-order, staggered-grid, finite-difference method. In this simulation, a rupture velocity of $v_r = 0.9\beta$ is assumed, where $\beta = 3.3$ km/s. The displacement distributions over a fault plane during rupture propagation can be visualized (Fig. 3).

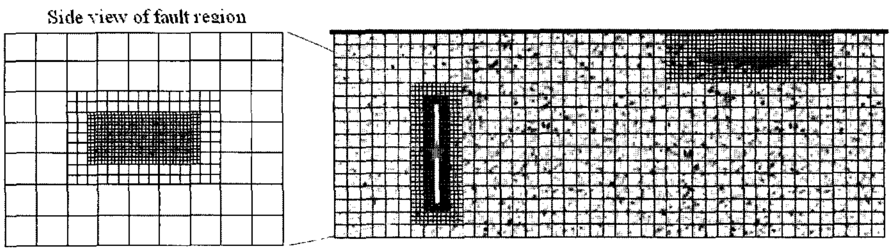

⟨Figure 2⟩ Model for simulating strong ground motion by dynamic rupture. Grids and time steps near the fault region are gradually refined in the same way as in the localized sedimentary basins.

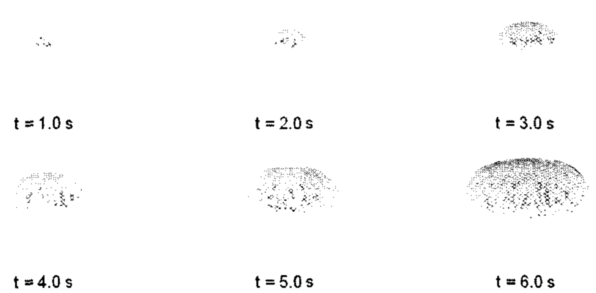

⟨Figure 3⟩ Displacement distributions over a fault plane during rupture propagation.

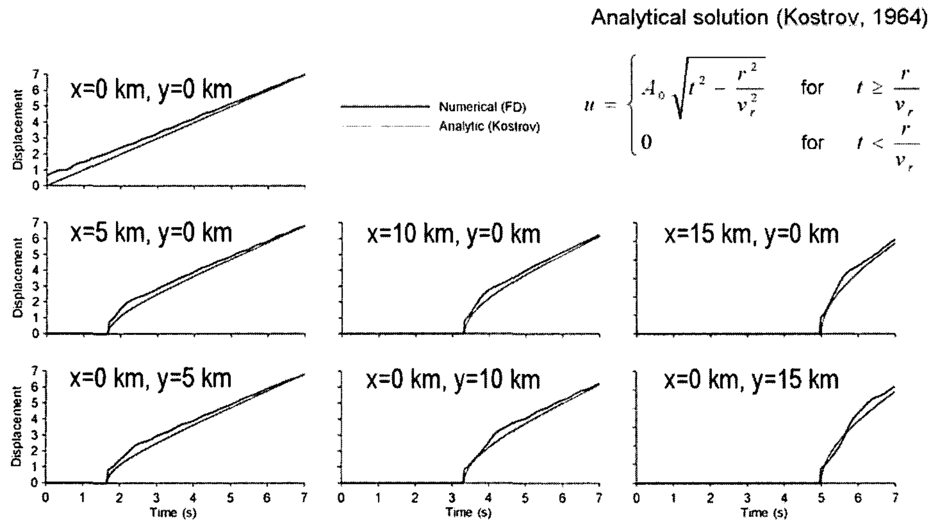

⟨Figure 4⟩ Displacements at several points on the fault plane depicted in Fig. 3. The numerical solution (blue line) is compared with the analytical solution (red line). The analytical solution is based on Kostrov (1964).

Kostrov (1964)[5] discussed the dynamics of crack extension for a semi-infinite longitudinal shear crack (e.g., Fig. 3). We compared our numerical results with Kostrov's self-similar solution to discuss the accuracy of the dynamic rupture model. Displacements at several points on the fault plane are shown in Fig. 4. Although the numerical solution involves minor oscillations, the agreement with Kostrov's results is satisfactory.

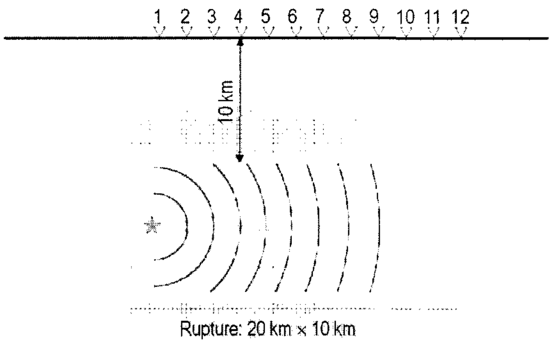

⟨Figure 5⟩ Gradually refined model of the fault zone. The prescribed fault boundary is indicated by a yellow line. Twelve observation points are located at the free surface to compare the results of the LVTS scheme with those of the CGTS scheme. Rupture initiates at the left end of the fault boundary, and the leading edge of rupture propagation is propagated circularly outward.

3.2 Gradually Refined Model of the Fault Zone

Dynamic rupture is simulated using localized discontinuous grids and a locally variable time step scheme. The fault plane is buried, and grids and time steps are gradually refined in the vicinity of the fault plane to a scale that is nine times finer than that in the outermost region (Fig. 5). The earthquake is represented as the propagation of stress relaxation over a prescribed finite fault plane. The fault rupture is assumed to propagate circularly at a prescribed velocity from an initial point on the fault plane. When the rupture front reaches any given point on the fault plane, shear stress drops to a prescribed frictional stress. The rupture stops abruptly when it reaches the prescribed fault boundary.

Ground velocity motions are calculated at several locations on the free surface. To investigate the validity and efficiency of the proposed approach, numerical results calculated using localized discontinuous grids in combination with the LVTS scheme were compared with those obtained using the constant grid and time steps (CGTS) finite-difference method. Table 1 indicates the numerical modeling parameters used in these simulations.

Figure 6 shows the simulation results recorded at the observation points indicated in Figure 5. The ground velocity at the free surface was calculated using the LVTS scheme. Seismic phases during rupture propagation are well resolved. To check the accuracy of the method, the results of the LVTS scheme were compared with those of the CGTS scheme. The two solutions are

〈Table 1〉 Comparison of Numerical Modeling Parameters for the Circular Rupture Simulation

	CGTS scheme	LVTS scheme
Temporal step (sec)	0.005	0.005 ~ 0.045
Spatial step (km)	0.125	0.125 ~ 1.125

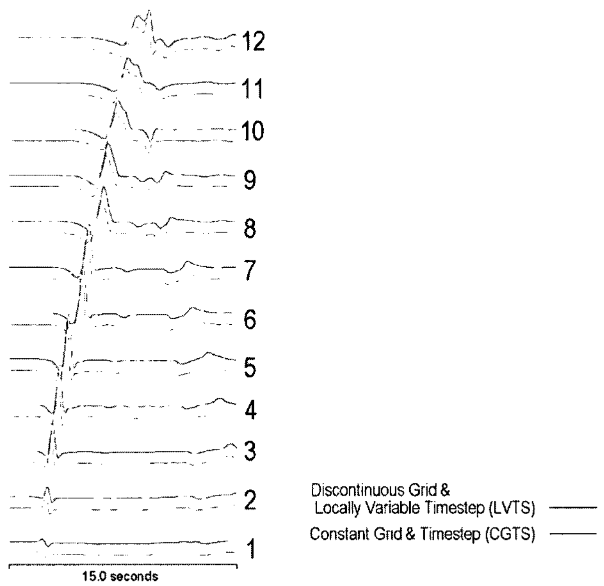

〈Figure 3〉 Ground velocities at the free surface for the gradually refined fault zone model. Observation locations are indicated in Fig. 5. Numerical results calculated using the LVTS scheme (blue line) are compared with those obtained using the CGTS scheme (red line).

in good agreement despite the slight phase difference. The LVTS scheme requires much larger grids and time steps than does the CGTS scheme (Fig. 5). In fact, the LVTS scheme is overwhelmingly advantageous in terms of its computational demands (Table 1; Kang and Baag 2004a).(2)

3.3 All-in-One Model

For the application of the proposed scheme, a more realistic situation is considered: a small basin in the Hongseong area, Korea. In the basin's bottom topography (Fig. 7), contours indicate the depth to bedrock (± 5 m). A region is delineated in which sampling parameters (Δh = 10.0 m, Δt = 0.002 sec) are three times finer than those of the surrounding region (Δh = 30.0 m, Δt = 0.006 sec). Details on the media parameters are the same as those in Kang and Baag (2004b).(3)

The simulation attempted to recreate the ground

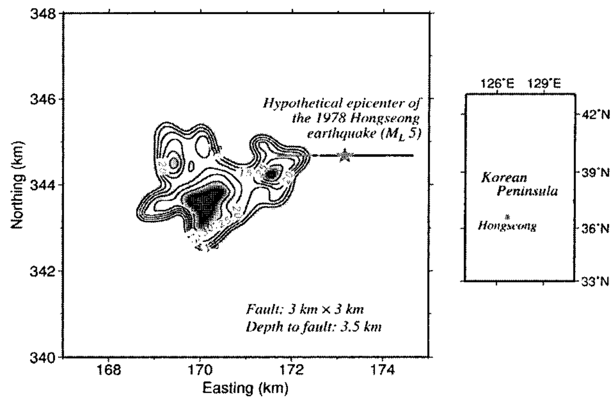

〈Figure 7〉 Basin bottom topography in the Hongseong area, Korea (Kang and Baag, 2004b). Contours show the distribution of depth to bedrock in a small-scale basin with depth interval of 5 meters. The thick line with a star indicates surface projection of the hypothetical fault plane of the 1978 Hongseong earthquake (M_L 5). The rectangle surrounding the basin denotes the region with grid and time steps that are three times finer than the rest of the region in the three-dimensional finite-difference simulation. A three-dimensional space near the fault plane has sampling parameters that are nine times finer (Δh = 3.33m, Δt = 0.00067 sec), with gradually increasing steps outside the fault plane.

motions in the basin caused by the 1978 Hongseong earthquake. In this small area, the exact epicenter of the earthquake cannot be resolved, so a hypothetical epicenter and earthquake fault plane without local geological consideration were used. A rectangular, east-trending, vertical, strike-slip fault plane 3 × 3 km in size is present at a depth of 3.5 km. A three-dimensional volume near the fault plane has sampling parameters nine times finer (Δh = 3.33 m, Δt = 0.00067 sec) than its surroundings. These modeling parameters ensure calculations of the wave field up to a frequency of 6 Hz. A rupture initiates at the center point of the fault plane and propagates circularly outward at a given velocity (v_r = 0.9β). Rupture propagation mechanisms are the same as those in the simulation for the gradually refined model discussed above.

Figure 8 shows the radial propagation of a wavefield initiated by dynamic rupture on the fault in the region with sampling parameters that are three times finer (Fig. 7, green rectangle). The snapshots depict the vertical component of velocity at 1-s intervals for the first 12 s after rupture initiation. After 12 s, the primary *S*-wave

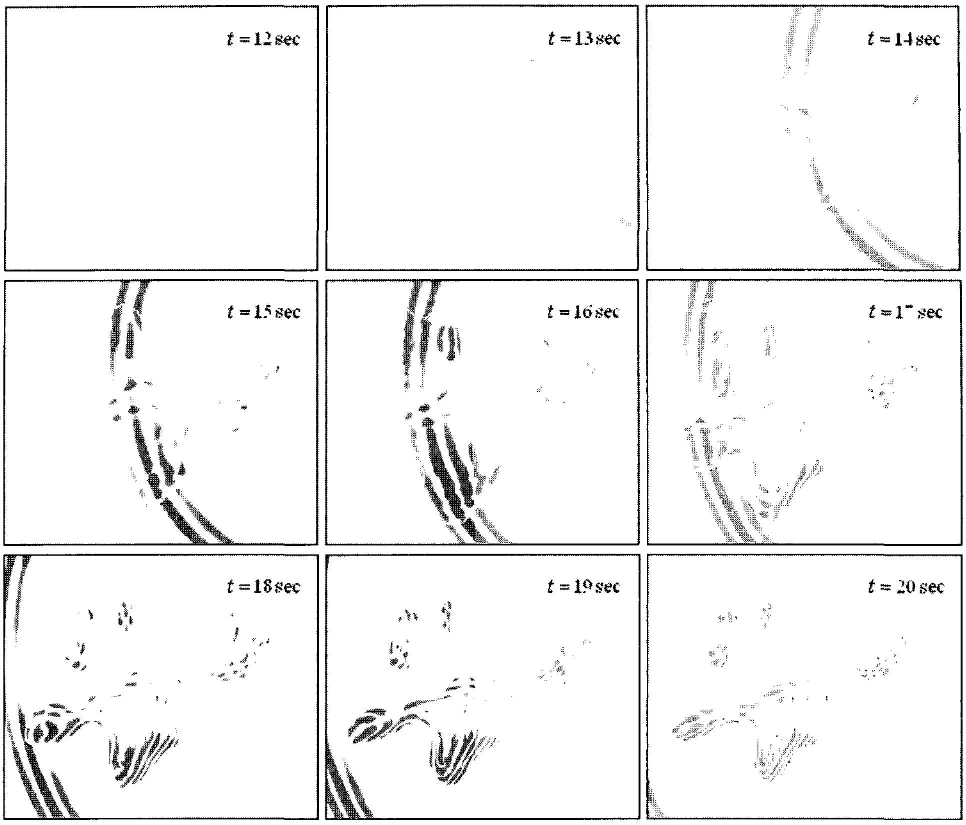

〈Figure 8〉 Snapshots of ground velocities radiated by dynamic rupture on the fault in the region with three-times finer sampling parameters (green rectangle in Fig. 7).

arrives at the right end of the basin at the free surface. As the primary *S*-wave sweeps the basin, more complex secondary waves are generated. These secondary waves are induced at the basin edge and are trapped within the basin, prolonging the duration of ground motion and amplifying the ground velocities. The amplification pattern of the ground motion is very complex in the basin. Qualitatively the ground motions are strongly amplified at the southwestern part of the basin and overall coincide with the thickness of the unconsolidated sedimentary layer. It is well known that sedimentary basins can significantly amplify earthquake ground motion, and the role of the basin response should be carefully considered in probabilistic seismic hazard analysis (e.g., Kawase 1996[(4)], Olsen and Archuleta 1996[(7)], Pitarka et al. 1996[(9)], Field et al. 2000[(1)]). Accordingly ground motion amplification with increased duration in the sedimentary basin could cause significant structural damage to the building environment in the Hongseong area even during the 1978 moderate-sized (M_L 5.0) Hongseong earthquake, which caused about 400 million won (about 400 thousand dollars) in damage as monetary value at that time.

4. DISCUSSION AND CONCLUSION

I presented a unified approach that incorporates multi-scale problems of dynamic rupture, radiated wave propagation, and site effects into an all-in-one model using a three-dimensional, fourth-order, staggered-grid, finite-difference method. Using a localized discontinuous grid scheme with locally variable time steps in the three-dimensional, fourth-order, finite-difference method, grid spacing and time steps near a fault plane can be progressively refined to preserve spatial resolution and low numerical dispersion. In this approach, any kind of dynamic fault model can be used, as long as it is implemented in the staggered-grid finite-difference method. The validity and efficiency of this approach was demonstrated through comparison with analytical solutions and with more conventional schemes. Simulation results for earthquake ground motion, including high-resolution rupture dynamics, were presented. Site effects and rupture processes are very important themes in the study of strong ground motion. An all-in-one model allows the consideration of the combined effects of these factors on earthquake ground responses. Comparing these types of simulation results with observational data on ground motion will provide a better understanding of the physical conditions influencing source dynamics. The proposed method makes it possible to understand strong ground motion as a product of a complex system and allows the possibility of a variety of fine-scale rupture scenarios and friction models. A series of deterministic earthquake scenarios may provide answers to the questions of what damage would result and where it would be located.

ACKNOWLEGMENT

This work was funded by the Korea Meteorological Administration Research and Development Program under Grant CATER 2006-5106.

REFERENCES

1. Field, E. H. and the SCEC Phase III Working Group, "Accounting for site effects in probabilistic seismic hazard analyses of southern California: overview of the SCEC Phase III Report", *Bulletin of the Seismological Society of America*, Vol. 90, No. 6B, 2000, pp. S1-S31.
2. Kang, T.-S. and Baag, C.-E., "Finite-difference seismic simulation combining discontinuous grids with locally variable timesteps", *Bulletin of the Seismological Society of America*, Vol. 94, No. 1, 2004a, pp. 207-219.
3. Kang, T.-S. and Baag, C.-E., "An efficient finite-difference method for simulating 3D seismic response of localized basin structures", *Bulletin of the Seismological Society of America*, Vol. 94, No. 5, 2004b, pp. 1690-1705.
4. Kawase, H., "The cause of the damaged belt zone: the basin-edge effect, constructive interference of the direct S-wave with the basin-induced diffracted / Rayleigh waves", *Seismological Research Letters*, Vol. 67, 1996, pp. 25-34.
5. Kostrov, B., "Self-similar problems of propagation of shear cracks", *Journal of Applied Mathematics and Mechanics*, Vol. 28, 1964, pp. 1077-1087.
6. Madariaga, R., Olsen, K. B. and Archuleta, R., "Modeling dynamic rupture in a 3D earthquake fault model", *Bulletin of the Seismological Society of America*, Vol. 88, 1998, pp. 1182-1197.
7. Olsen, K. B. and Archuleta, R. J., "Three-dimensional simulation of earthquake on the Los Angeles fault system", *Bulletin of the Seismological Society of America*, Vol. 86, 1996, pp. 575-596.
8. Panza, G. F., Romanelli, F., Vaccari, F., Decanini, L. and Mollaioli, F., "Seismic ground motion modeling and damage earthquake scenarios: a possible bridge between seismologists and seismic engineers", in *Earthquake Hazard, Risk and Strong Ground Motion*, edited by Chen, Y. T., Panza, G. F. and Wu, Z. L., Seismological Press, Beijing, China, 2004, pp. 323-349.
9. Pitarka, A., Irikura, K., Iwata, T. and Kagawa, T., "Basin structure effects in the Kobe area inferred from the modeling of ground motions from two aftershocks of the January 17, 1995 Hygoken-nambu earthquake", *Journal of Physics of the Earth*, Vol. 44, 1996, pp. 563-576.